THE JOURNAL OF PHYSICAL CHEMISTRY Letters

Letter

pubs.acs.org/JPCL

Spin-Noise-Detected Two-Dimensional Fourier-Transform NMR Spectroscopy

Kousik Chandra,[†] Judith Schlagnitweit,[†,§] Christian Wohlschlager,[‡] Alexej Jerschow,[⊥] and Norbert Müller*[,†]

[†]Institute of Organic Chemistry and [‡]Scientific Computing Department, Johannes Kepler University Linz, Altenbergerstraße 69, Linz 4040, Austria

[⊥]Department of Chemistry, New York University, 100 Washington Square East, New York 10003, United States

Supporting Information

ABSTRACT: We introduce two-dimensional NMR spectroscopy detected by recording and processing the noise originating from nuclei that have not been subjected to any radio frequency excitation. The method relies on cross-correlation of two noise blocks that bracket the evolution and mixing periods. While the sensitivity of the experiment is low in conventional NMR setups, spin-noise-detected NMR spectroscopy has great potential for use with extremely small numbers of spins, thereby opening a way to nanoscale multidimensional NMR spectroscopy.

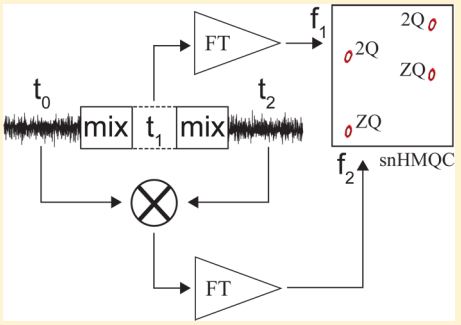

SECTION: Spectroscopy, Photochemistry, and Excited States

Felix Bloch predicted the existence of spin-noise in 1946.[1] Experimental verification had to wait until 1985[2] due to the low amplitude of the phenomenon. Recent progress in magnetic resonance instrumentation, in particular, cryogenically cooled probes[3] and force-detected magnetic resonance as well as extensive work on one-dimensional spin-noise spectroscopy,[4−8] has opened new possibilities for in-depth investigation of the physical phenomenon and the exploration of its application potential. For a recent review, see ref 9.

In the present context, we focus on the transverse components of spin-noise as opposed to the longitudinal component, which is exploited in the force-detected magnetic resonance experiments.[5] The fluctuating transverse spin-noise exhibits random phase contributions, which average to zero with the transverse relaxation time constant of T_2 (or T_2* if inhomogeneous broadening prevails). Noise blocks therefore would have an expectation value of zero due to cancellations, but averaging over the signal magnitude or power can be used for signal accumulation. The earlier described spin-noise spectroscopy[10−16] and imaging experiments[17] were obtained by Fourier-transforming individual noise blocks and co-adding the magnitude or power representations of these data. This is equivalent to computing the Fourier-transform of the autocorrelation of the spin-noise as described by the Wiener−Khintchine theorem (WKT).[18,19] Both procedures can be used for signal accumulation by avoiding cancellations due to the random phases that are exhibited by the (uncorrelated) noise signals.

To obtain two-dimensional Fourier-transform spin-noise NMR spectra, we use the following basic concept, illustrated in Figure 1.

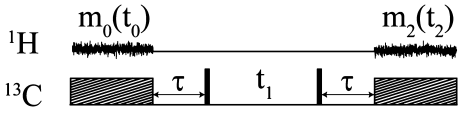

Figure 1. Acquisition scheme for noise-detected two-dimensional NMR. The general scheme consists of an evolution time t_1 sandwiched between two mixing periods τ_1 and τ_2 and two noise acquisition periods t_0 and t_2, during which the noise blocks $m_0(t_0)$ and $m_2(t_2)$ are acquired in an identical manner. In the spin-noise-HMQC (snHMQC) pulse sequence, used to demonstrate and test the concept of spin-noise-detected two-dimensional NMR spectra, black rectangular bars represent 90°$_x$ hard pulses on the ^{13}C channel. The hatched rectangles represent periods of heteronuclear decoupling (WALTZ). No pulses are applied on the ^{1}H channel.

Two noise blocks, $m_0(t_0)$ and $m_2(t_2)$, are recorded in identical fashion similar to the CONQUEST paradigm.[5,20] Between the two noise blocks, one places an evolution period, as usual in multidimensional NMR, bracketed by two mixing periods. Cross-correlating the time domain noise blocks $m_0(t_0)$ with $m_2(t_2)$ for each t_1 value yields a conventional two-dimensional time domain NMR data set that can be processed in the usual manner. It is however crucial that the cross-correlation (either in the time or frequency domain) is performed prior to signal averaging. The experiment depicted in Figure 1, as a first demonstration of the principle of indirect

Received: September 29, 2013
Accepted: October 29, 2013
Published: October 29, 2013

   dx.doi.org/10.1021/jz402100g | J. Phys. Chem. Lett. 2013, 4, 3853−3856

detection by spin-noise, correlates spin-noise-detected ^{1}H chemical shifts with heteronuclear multiple-quantum coherence without applying any rf pulses on the ^{1}H channel, henceforth called a ^{1}H spin-noise-HMQC (snHMQC) experiment. We use the symbols I and S for the nuclei ^{1}H and ^{13}C, respectively, in the following analysis. During the first acquisition period t_0, a ^{1}H noise block m_0 is recorded, while decoupling the S spins, and the recorded signal can be described as

$$m_0(t_0) = \int_{-\infty}^{t_0} a_0(t_a) e^{-i\Omega_I(t_0-t_a)-R_2(t_0-t_a)}\, dt_a + n_0(t_0) \quad (1)$$

where $a_0(t_a)$ describes the complex-valued random emission amplitude of an emission event (we do not distinguish between induced and spontaneous emission in the present context) at time point t_a, Ω_I is the I-spin resonance frequency, $R_2 = 1/T_2$ or $1/T_2^*$ depending on which regime applies, and $n_0(t_0)$ is the background broad-band noise (which may be assumed to be white noise over the observed spectral width) amplitude from the instrument or other sources. Heteronuclear decoupling of spin-noise signals works as expected; therefore, there is no coupling modulation in eq 1. It was shown previously that heteronuclear decoupling does not cause spectral interference with the hardware used.[16]

At the end of this first acquisition interval, t_0 decoupling is turned off, and the surviving coherences arising from the incomplete cancellation of spin-noise transverse components start evolving under heteronuclear coupling constant J_{IS}. At the end of the $\tau_1 = (2J_{IS})^{-1}$ period, heteronuclear antiphase coherence is generated. The 90° pulse on the S channel transforms it into a superposition of two spin coherences (double- and zero-quantum coherences), which evolve during t_1. The second 90° pulse regenerates antiphase I-spin single-quantum coherence, which is refocused to in-phase transverse magnetization in the second delay $\tau_2 = (2J_{IS})^{-1}$. Focusing on the pathways of interest, the measured signal during the t_2 period can be written as

$$\begin{aligned} m_2(t_2) = {} & f(\tau_1, \tau_2)\{e^{-i(\Omega_I+\Omega_S)t_1-R_{DQ}t_1} \\ & + e^{-i(\Omega_I-\Omega_S)t_1-R_{ZQ}t_1}\}e^{-i\Omega_I(\tau_1+\tau_2)-i\Omega_I t_2-R_2 t_2} \\ & \times \int_{-\infty}^{t_0^{max}} a_0(t_a) e^{-i\Omega_I(t_0^{max}-t_a)-R_2(t_0^{max}-t_a)}\, dt_a \\ & + b(\tau_1, \tau_2, t_1) e^{-i\Omega_I t_2-R_2 t_2} \\ & + \int_0^{t_2} c(t_c) e^{-i\Omega_I(t_2-t_c)-R_2(t_2-t_c)}\, dt_c + n_2(t_2) \end{aligned} \quad (2)$$

where t_0^{max} is the maximum acquisition time, which is equal for the periods t_0 and t_2 in this experiment, and Ω_S is the Larmor frequency of spin S. The transfer coefficient $f(\tau_1, \tau_2)$ includes the effects of deviations from ideally matched delays. R_{DQ} and R_{ZQ} are the double- and zero-quantum relaxation rates, respectively, $n_2(t_2)$ is the background noise amplitude from the instrument or other sources, b represents the contributions to the signal from the emission events occurring in the period between the two direct acquisition periods t_0 and t_2, and the integral encompassing c represents contributions to the signal from emission events originating at time t_c within the t_2 period. Decoupling of the S spins is switched on during t_0 and t_2. Hence, there is no coupling evolution during this period.

The desired signals can now be "distilled" from the data in the two measurement blocks by calculating the correlation function $m_0(t_0) \otimes m_2(t_2)$. It is convenient to calculate the Fourier-transform of this correlation function because by the WKT, it is equal to the product of the Fourier-transforms of the time domain functions

$$G(\Omega) = \mathrm{FT}\{m_0(t_0) \otimes m_2(t_2)\} = M_0^*(\Omega)M_2(\Omega) \quad (3)$$

where FT symbolizes the Fourier-transform, and we use the common convention that capital letter variables with angular frequency arguments represent the Fourier-transforms of the corresponding lowercase quantities.

Because m_0 and the desired "a" signals in m_2 are themselves convolutions (WKT), their Fourier-transforms are found readily as

$$M_0(\Omega) = A_0(\Omega)L(R_2, \Omega - \Omega_I) + N_0(\Omega) \quad (4)$$

and

$$\begin{aligned} M_2(\Omega) = {} & L(R_2, \Omega - \Omega_I)\{A_0(\Omega)f(\tau_1, \tau_2)e^{-i\Omega_I(\tau_1+\tau_2+t_0^{max})} \\ & \times\{e^{-i(\Omega_I+\Omega_S)t_1-R_{DQ}t_1} + e^{-i(\Omega_I-\Omega_S)t_1-R_{ZQ}t_1}\} + b(\tau_1, \tau_2, t_1) \\ & + C(\Omega)\} + N_2(\Omega) \end{aligned} \quad (5)$$

with L being the complex Lorentzian line shape function

$$L(R, Q) = \frac{1}{R + i\Omega} \quad (6)$$

We then obtain for the Fourier-transform of the correlation function

$$\begin{aligned} G(\Omega) = {} & |A_0(\Omega)|^2|L(R_2, \Omega - \Omega_I)|^2 f(\tau_1, \tau_2)e^{-i\Omega_I(\tau_1+\tau_2+t_0^{max})} \\ & \times\{e^{-i(\Omega_I+\Omega_S)t_1-R_{DQ}t_1} + e^{-i(\Omega_I-\Omega_S)t_1-R_{ZQ}t_1}\} \\ & + |L(R_2, \Omega - \Omega_I)|^2 A_0(\Omega)(b(\tau_1, \tau_2, t_1) + C(\Omega)) \\ & + L(R_2, \Omega - \Omega_I)(A_0(\Omega)N_2(\Omega) \\ & + A_0(\Omega)N_0(\Omega)f(\tau_1, \tau_2)e^{-i\Omega_I(\tau_1+\tau_2+t_0^{max})}\{e^{-i(\Omega_I+\Omega_S)t_1-R_{DQ}t_1} \\ & + e^{-i(\Omega_I-\Omega_S)t_1-R_{ZQ}t_1}\}) \\ & + \text{cross-terms between } N_0 \text{ and } N_2(\Omega),\ b,\ C \end{aligned} \quad (7)$$

The cross-terms between the A, b, C, and the different N terms are completely uncorrelated and can be averaged out to arbitrary precision by accumulating the cross-correlation function (or its Fourier-transform) over many acquisitions. Only the first summand in eq 7, which contains the square of the random amplitude $|A_0(\Omega)|^2$ and represents the correlated signals, increases linearly with the number of co-added cross-correlated data blocks. The uncorrelated terms (the other summands) only grow with the square root of this number. A further Fourier-transform with respect to t_1 gives the correlation peaks of interest in the form

$$\begin{aligned} G(\Omega_1, \Omega_2) = {} & |A_0(\Omega)|^2|L(R_2, \Omega_2 - \Omega_I)|^2 f(\tau_1, \tau_2) \\ & \times e^{-i\Omega_I(\tau_1+\tau_2+t_0^{max})}\{L(R_{DQ}, \Omega_1 - \Omega_I - \Omega_S) \\ & + L(R_{ZQ}, \Omega_1 - \Omega_I + \Omega_S)\} \end{aligned} \quad (8)$$

where we have neglected the cross-terms and used the correspondence $\Omega_2 = \Omega$ to conform with multidimensional NMR conventions. It is seen here that heteronuclear cross-peaks are obtained at the coordinates $(\Omega_I \pm \Omega_S, \Omega_I)$, as expected.

In Figure 2, we show an experimental two-dimensional snHMQC spectrum of ^{13}C-enriched glucose acquired with the scheme of Figure 1 and processed using a TopSpin 3.1

dx.doi.org/10.1021/jz402100g | J. Phys. Chem. Lett. 2013, 4, 3853−3856

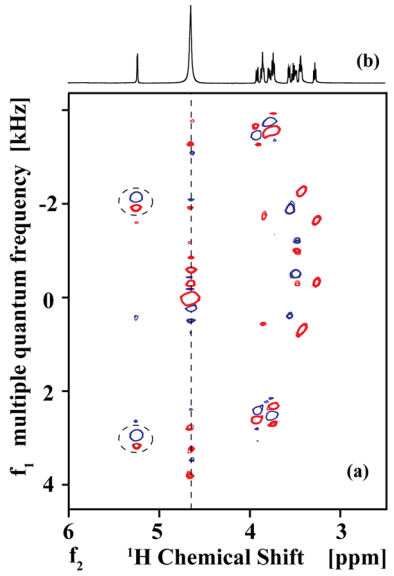

Figure 2. (a) Spin-noise-detected two-dimensional HMQC (snHMQC) spectrum of 99% ^{13}C-enriched glucose in $^{2}H_2O$. For the spectrum shown here, 6000 passes were co-added. Processing is described in the text. The dashed vertical line indicates the position of the $^{1}HO^{2}H$-t_1 noise artifacts. The two circled regions illustrate the positions of the zero- and double-quantum coherence cross-peaks of the anomeric C−H positioned at $f_1 = \Omega_{H\text{-}1} \pm \Omega_{C\text{-}1}$, $f_2 = \Omega_H$, respectively. Red and blue contour lines represent positive and negative levels, respectively. The residual solvent signal gives rise to a peak at zero frequency in f_1, and several truncation artifacts are visible at that frequency due to the short maximum evolution time. (b) A ^{13}C decoupled ^{1}H single pulse spectrum is shown for reference.

"au"-program (written in C) and a Matlab script implementing eqs 7 and 8, all available in the Supporting Information.

The spectrum has been acquired with low resolution in both dimensions in order to reduce relaxation losses. As predicted above, two cross-peaks are observed for each ^{1}H resonance, corresponding to the heteronuclear zero- and double-quantum frequencies. The spectrum is phase-sensitive in the indirect dimension, while in the direct dimension, only a real part exists. In the f_1 dimension, peak splitting occurs due to homonuclear carbon and proton couplings. Due to the evolution of chemical shifts and spin−spin couplings prior to the indirect detection period t_1, a mixed phase spectrum is obtained with the pulse scheme in Figure 1.

The fact that spin-noise can have an effect strong enough to drive a two-dimensional coherence transfer experiment will come as a surprise for many readers. Therefore, in the Supporting Information, we give an estimate of the magnitude of the spin-noise signal under the conditions of our experiment in Figure 2, following the basic ideas by Guéron and Leroy[11] as well as Hoult and Ginsberg.[21] It should also be mentioned that stochastic excitation for obtaining two-dimensional correlation NMR spectra, albeit using a pseudorandom number generator to drive the rf excitation pulses, has been introduced by Blümich and co-workers earlier.[22,23]

Because the repetition interval of spin-noise-detected experiments is completely independent of the ^{1}H longitudinal relaxation time T_1, the acquisition schemes can be repeated as fast as the hardware allows. Still, the per root-of-transient-number signal-to-noise ratio in the spectra obtained is very low compared to pulse excitation spectra because the separation of the small amount of correlated noise from uncorrelated noise depends on the amount of signal averaging. Several enhancements to the efficiency of the acquisition scheme are currently under investigation. However, one should bear in mind that by extrapolating to lower spin numbers, noise power amplitudes will exceed pulse excitation amplitudes originating from natural polarization.[17,24]

On the basis of the noise-correlation principle outlined here, a large range of multidimensional magnetic resonance experiments becomes feasible. In principle, any coherence transfer pulse sequence can be modified accordingly as long as the relaxation times permit. In a potential application at the nanoscale, that is, below ~10^8 nuclear spins, application of rf pulses, in particular, refocusing pulses, on the detection channel will also be possible because the magnitude of the residual coherence generated will be below the thermal Curie law polarization. Thus, we expect substantial future developments of spin-noise-detected MR techniques at the nanoscale, which will not be restricted to heteronuclear correlation. The paradigm of detection through correlated spin-noise may very likely also find useful applications in optically detected NMR spectroscopy, in particular, diamond-NV-center experiments,[25−28] and could also be implemented in optical multidimensional noise spectroscopy.[29,30]

EXPERIMENTAL METHODS

The experiments were performed on a 700 MHz Bruker Avance III system equipped with a TCI cryo-probe. The spin-noise-detected two-dimensional HMQC (snHMQC) spectrum shown was recorded on 99% ^{13}C-enriched glucose in $^{2}H_2O$ (0.648 mol L^{-1}) in a 5 mm NMR tube using the scheme of Figure 1, with the following parameters: $t_0 = t_2 = 27$ ms, ^{1}H spectral width 9.5 kHz, maximum $t_1 = 3.78$ ms, ^{13}C spectral width 10.6 kHz, 90°(^{13}C) pulse 12.6 μs, repetition delay 250 ms. The mixing times τ were 1.72 ms. One pass through all 80 t_1 values of the sequence thus takes 27 s. Because no refocusing pulses could be used on the ^{1}H channel (to avoid generation of spurious coherence), all acquisition and evolution times are generally short as T_2* rather than T_2 determines the loss of coherence in this particular experiment. For the spectrum shown in Figure 2, 6000 passes through the pulse sequence were co-added. Processing is described in the text. The $^{2}H_2O$ deuterium signal was used for field frequency locking.

To process the data, TopSpin 3.1 C-programs and Matlab scripts, which are available in the Supporting Information, were used. First, Fourier-transformation along the direct dimension was performed in TopSpin 3.1 (by the command xf2). Then, the cross-correlation of the two noise blocks, m_0 and m_2, for each t_1 time point was achieved by an in-house written "au"-program multiplying the transformed data blocks, point by point (see eq 3). Fourier-transformation along the indirect t_1 dimension and addition of 6000 different experiments were done using a Matlab script.

ASSOCIATED CONTENT

Supporting Information

Estimate of the magnitude of the spin-noise signal (Text S1), Bruker pulse program (for Topspin 3.1) for snHMQC (Text S2) as well as the "au"-program (Text S3) and Matlab scripts (Text S4) for processing of the snHMQC data. This material is available free of charge via the Internet at http://pubs.acs.org.

AUTHOR INFORMATION

Corresponding Author

*E-mail: norbert.mueller@jku.at. Phone: +43 732 2468 8746.

Present Address
[§]J.S.: Université de Lyon (ENS Lyon/CNRS/UCB Lyon 1), Centre de RMN à très hauts champs, 69100, Villeurbanne, France.

Notes
The authors declare no competing financial interest.

■ ACKNOWLEDGMENTS

The research reported was supported in part by the Austrian Science Funds FWF (Projects M1404 for K.C. and N.M. and Project I1115-N19 for N.M.), as well as by the European Union through the EFRE INTERREG IV (ETC-AT-CZ) program (Project M00146 "RERI-uasb" for N.M.) and via FP7 EAST-NMR, Contract No. 228461. A.J.'s effort was supported by a US NSF grant CHE 0957586. We are grateful to Dr. Wolfgang Bermel (Bruker-BioSpin, Germany) for support in programming within the TopSpin environment. N.M. dedicates this Research Report with gratitude to Prof. Richard R. Ernst on the occasion of his 80[th] birthday.

■ REFERENCES

(1) Bloch, F. Nuclear Induction. *Phys. Rev.* **1946**, *70*, 460−475.
(2) Sleator, T.; Hahn, E. L.; Hilbert, C.; Clarke, J. Nuclear-Spin Noise. *Phys. Rev. Lett.* **1985**, *55*, 1742−1746.
(3) Kovacs, H.; Moskau, D.; Spraul, M. Cryogenically Cooled Probes—A Leap in NMR Technology. *Prog. Nucl. Magn. Reson. Spectrosc.* **2005**, *46*, 131−155.
(4) Degen, C. L.; Poggio, M.; Mamin, H. J.; Rettner, C. T.; Rugar, D. Nanoscale Magnetic Resonance Imaging. *Proc. Natl. Acad. Sci. U.S.A.* **2009**, *106*, 1313−1317.
(5) Madsen, L. A.; Leskowitz, G. M.; Weitekamp, D. P. Observation of Force-Detected Nuclear Magnetic Resonance in a Homogeneous Field. *Proc. Natl. Acad. Sci. U.S.A.* **2004**, *101*, 12804−12808.
(6) Crooker, S. A.; Rickel, D. G.; Balatsky, A. V.; Smith, D. L. Spectroscopy of Spontaneous Spin Noise as a Probe of Spin Dynamics and Magnetic Resonance. *Nature* **2004**, *431*, 49−52.
(7) Mamin, H. J.; Budakian, R.; Chui, B. W.; Rugar, D. Magnetic Resonance Force Microscopy of Nuclear Spins: Detection and Manipulation of Statistical Polarization. *Phy. Rev. B* **2005**, *72*, 0244131−0244136.
(8) Jurkiewicz, A. The Observation and Dynamics of ^{1}H NMR Spin Noise in Methanol. *Appl. Magn. Reson.* **2013**, *44*, 1181−1198.
(9) Müller, N.; Jerschow, A.; Schlagnitweit, J. Nuclear Spin Noise. *eMagRes* **2013**, *2*, 237−244.
(10) McCoy, M. A.; Ernst, R. R. Nuclear Spin Noise at Room Temperature. *Chem. Phys. Lett.* **1989**, *159*, 587−593.
(11) Guéron, M.; Leroy, J. L. NMR of Water Protons. The Detection of Their Nuclear-Spin Noise, and a Simple Determination of Absolute Probe Sensitivity Based on Radiation Damping. *J. Magn. Reson.* **1989**, *85*, 209−215.
(12) Marion, D. J.-Y.; Desvaux, H. An Alternative Tuning Approach to Enhance NMR Signals. *J. Magn. Reson.* **2008**, *193*, 153−157.
(13) Nausner, M.; Schlagnitweit, J.; Smrecki, V.; Yang, X.; Jerschow, A.; Müller, N. Non-Linearity and Frequency Shifts of Nuclear Magnetic Spin-Noise. *J. Magn. Reson.* **2009**, *198*, 73−79.
(14) Schlagnitweit, J.; Dumez, J.-N.; Nausner, M.; Jerschow, A.; Elena-Herrmann, B.; Müller, N. Observation of NMR Noise from Solid Samples. *J. Magn. Reson.* **2010**, *207*, 168−172.
(15) Giraudeau, P.; Müller, N.; Jerschow, A.; Frydman, L. ^{1}H NMR Noise Measurements in Hyperpolarized Liquid Samples. *Chem. Phys. Lett.* **2010**, *489*, 107−112.
(16) Schlagnitweit, J.; Müller, N. The First Observation of C-13 Spin Noise Spectra. *J. Magn. Reson.* **2012**, *224*, 78−81.
(17) Müller, N.; Jerschow, A. Nuclear Spin Noise Imaging. *Proc. Natl. Acad. Sci. U.S.A.* **2006**, *103*, 6790−6792.
(18) Khintchine, A. Korrelationstheorie der stazionären stochastischen Prozesse. *Math. Ann.* **1934**, *109*, 604−615.
(19) Wiener, N. Generalized Harmonic Analysis. *Acta Math.* **1930**, *55*, 117−258.
(20) Carson, P. L.; Leskowitz, G. M.; Madsen, L. A.; Weitekamp, D. P. Method for Suppressing Noise in Measurements. U.S. Patent 6078872 A, October 19, 1999.
(21) Hoult, D. I.; Ginsberg, N. S. The Quantum Origins of the Free Induction Decay Signal and Spin Noise. *J. Magn. Reson.* **2001**, *148*, 182−199.
(22) Blümich, B.; Kaiser, R. Stochastic NMR on a Commercial Spectrometer. *J. Magn. Reson.* **1984**, *58*, 149−151.
(23) Blümich, B.; Ziessow, D. 2D NMR-Spectra from Stochastic NMR — Coupling and Exchange Information from 3rd Order Frequency Kernel. *Ber. Bunsen-Ges. Phys. Chem* **1980**, *84*, 1090−1102.
(24) Sleator, T.; Hahn, E. L.; Hilbert, C.; Clarke, J. Nuclear-Spin Noise and Spontaneous Emission. *Phys. Rev. B* **1987**, *36*, 1969−1980.
(25) Mamin, H. J.; Kim, M.; Sherwood, M. H.; Rettner, C. T.; Ohno, K.; Awschalom, D. D.; Rugar, D. Nanoscale Nuclear Magnetic Resonance with a Nitrogen-Vacancy Spin Sensor. *Science* **2013**, *339*, 557−560.
(26) Staudacher, T.; Shi, F.; Pezzagna, S.; Meijer, J.; Du, J.; Meriles, C. A.; Reinhard, F.; Wrachtrup, J. Nuclear Magnetic Resonance Spectroscopy on a (5-Nanometer)^{3} Sample Volume. *Science* **2013**, *339*, 561−563.
(27) Zapasskii, V. S.; Greilich, A.; Crooker, S. A.; Li, Y.; Kozlov, G. G.; Yakovlev, D. R.; Reuter, D.; Wieck, A. D.; Bayer, M. Optical Spectroscopy of Spin Noise. *Phys. Rev. Lett.* **2013**, *110*, 176601.
(28) Fink, T.; Bluhm, H. Noise Spectroscopy Using Correlations of Single-Shot Qubit Readout. *Phys. Rev. Lett.* **2013**, *110*, 010403.
(29) Turner, D. B.; Howey, D. J.; Hendrickson, R. A.; Gealy, M. W.; Sutor, E. J.; Ulness, D. J. Two-dimensional electronic spectroscopy using incoherent light: theoretical analysis. *J. Phys. Chem. A* **2013**, *117*, 5926−5954.
(30) Turner, D. B.; Arpin, P. C.; McClure, S. D.; Ulness, D. J.; Scholes, G. D. Coherent multidimensional optical spectra measured using incoherent light. *Nat. Comm.* **2013**, *4*, 2298.